I.J. Image, Graphics and Signal Processing, **2026, 5, 93-109**
Published Online on October 8, 2026 by MECS Press (http://www.mecs-press.org/)
DOI: 10.5815/ijigsp.2026.05.06

PLL based IRNSS Signal Tracking using Real Time Data

Kavita Guddad*
Department of Electronics and Communication Engineering, Dayananda Sagar College of Engineering, Bengaluru, India
E-mail: kavita-ece@dayanandasagar.edu
ORCID iD: https://orcid.org/0009-0005-8027-9623
*Corresponding author

K. L. Sudha
Department of Electronics and Communication Engineering, Dayananda Sagar College of Engineering, Bengaluru, India
E-mail: drsudha-ece@dayanandasagar.edu
ORCID iD: https://orcid.org/0000-0001-8301-1669

Received: February 9, 2026; Revised: March 5, 2026; Accepted: July 9, 2026; Published: October 8, 2026

Abstract: The need for flexible software receivers for research and experimentation has naturally grown due to the rapid development of Global/Regional Navigation Satellite System (GNSS/RNSS) constellations, created to cater to the navigation requirements of various countries. The two primary functions of all such receivers are signal acquisition and signal tracking. One must have a firm understanding of these functions to design or improve an existing navigation receiver. Signal acquisition is the first operation at the receiver, after filtering the received signal to remove noise. It provides the preliminary estimates of the carrier frequency and code phase and assists in identifying the satellites that are in view of the receiver. The accuracy of these estimates is then progressively improved by tracking. To accomplish this refinement using a correlation operation to compare the received signal and locally generated code and carrier replicas, the tracking process uses a tracking loop whose main part is a Phase-Locked Loop (PLL). This step is especially crucial because it eliminates the modulation that was added at the transmitter, enabling the receiver to retrieve the navigational information required for position calculation. The PLL continuously modifies the locally generated code and carrier replicas based on the discriminator output to maintain alignment with the incoming signal. The correlation peaks, when the local replicas and the received signal are well synchronized, showing the effective cancellation of the code and carrier modulation. This makes it possible to reliably extract the navigation message. Using GPS as the reference model, we present in this work a thorough explanation of the tracking mechanism, the structure of the PLL, and the mathematical principles governing its operation. The Indian Regional Navigation Satellite System (IRNSS) signal structure is then subjected to the same methodology. To validate the method we have used the actual intermediate-frequency data from an IRNSS-User Receiver (IRNSS-UR) installed by ISRO at the IRNSS lab of Jain University, Bengaluru. The obtained values of frequency and phase jitter to measure the performance of the tracking loop show that the tracking loop is stable.

Index Terms: GNSS, IRNSS, Signal Tracking, Satellite Navigation, Phase-Locked Loop.

1. Introduction

Today's navigation, positioning, and timing services heavily depend on GNSS/RNSS. The low-rate navigation data that constitutes a typical GNSS signal is modulated twice before being sent from the satellite. The first modulation is Direct Sequence Spread Spectrum (DSSS) which spreads the data providing improved resistance to interferences. The spreading is accomplished by multiplying the navigation bits with a Pseudo Random Noise (PRN) sequence typically derived from Gold codes. In the second modulation the spread signal modulates a radio-frequency carrier, most of the time using digital binary phase modulation i.e. BPSK, to create a waveform that can withstand propagation losses and atmospheric attenuation during its travel through air to the receiver.

Signal acquisition and signal tracking are two core operations of every GNSS/RNSS receiver. By locating visible satellites and generating rough estimates of the carrier frequency and code phase, acquisition provides the initial stage

This work is open access and licensed under the Creative Commons CC BY 4.0 License.

of synchronization. Even though they are rough, these preliminary estimates are necessary to allow the receiver to move on to the more difficult task of tracking. Even in the presence of Doppler variations, code delays, channel noise, and numerous other distortions, tracking consistently improves these estimates and keeps the arriving signal in stable alignment. The precision and resilience of this tracking phase are critical to the receiver's capacity to retrieve the navigation message and confidently ascertain the user's location.

The received signal includes both the channel noise due to transmission in the medium and the noise introduced at the satellite transmitter. Hence the noise must be suppressed by appropriate filtering and the applied modulations must be carefully reversed by the receiver in order to recover the embedded navigation data. This is achieved by both acquisition and tracking [1], but tracking is especially important as it eliminates the code and carrier modulation effects added at the transmitter and makes the navigation message readable [2].

This work provides a thorough knowledge about the signal-tracking procedure, considering GPS framework and applying the same ideas to IRNSS signals. A thorough description of the Phase-Locked Loop (PLL) design, the tracking loop architecture, along with the underlying mathematical formulation is presented. Real IF data recorded by an IRNSS-User Receiver (IRNSS-UR) deployed by ISRO at the IRNSS laboratory in Jain University, Bengaluru, are utilized to assess the performance of the suggested technique. The experimental results confirm the efficacy of the tracking process and offer a solid foundation for upcoming developments in GNSS/IRNSS receiver technology.

2. Literature Review

This section outlines a few representative contributions of the substantial research done on various elements of the GNSS tracking process, ranging from its mathematical foundations to its influence on positioning accuracy and the benefits of combining multiple constellations.

Research paper [3] by Pany et al. contains a comprehensive survey of the evolution of Software-defined GNSS receivers which have gradually become central to navigation-signal experimentation, as they provide unrestricted access to digitized IF samples and allow researchers to adjust or redesign tracking algorithms with relative ease. In this work the authors trace the field from early MATLAB-based prototypes—often slow and limited in scope—to today's real-time platforms that support multi-constellation signal processing, hardware acceleration, and active community-driven development. Carrier tracking, in particular, continues to receive considerable attention, as it is responsible for keeping the phase of the local carrier replica in alignment with the incoming satellite signal.

Stevanović's work in [4] offers a detailed treatment of PLL behavior. The study discusses lock thresholds, noise-induced phase variability, and the loop's ability to endure interference, all framed through rigorous statistical modeling, and later refinements, including INS-assisted PLLs, add external motion cues to stabilize the loop during rapid dynamics or ionospheric disturbances. These studies provide a strong analytical basis for choosing loop order, discriminator type, and bandwidth choices that are especially significant in IRNSS applications, where the L5 and S-band signals have propagation characteristics that differ from those of other GNSS systems.

More advanced tracking strategies, such as vector tracking, have also gained attention. These architectures jointly process measurements from multiple satellites and integrate the tracking operations with the navigation filter. As a result, vector tracking tends to be more resilient in low C/N_0 conditions and can maintain continuity through short signal blockages [5]. Variants like quasi-open-loop tracking further reduce latency in the feedback path, which in turn helps to suppress the phase jitter without compromising stability. Such features are particularly relevant for IRNSS as the regional variations in signal availability make continuous and robust tracking an operational priority.

As the IRNSS system has moved towards full operational use, the research focus on NavIC/IRNSS also has grown rapidly. Studies describing the L5 and S-band signals outline details such as the Gold-code structure, BPSK modulation, and the non-uniform distribution of received power across the coverage area. Several authors have proposed acquisition and tracking algorithms tailored to these signals, noting contrasts with GPS in terms of Doppler behavior, code properties, and channel conditions. Experimental investigations using real IF recordings including datasets captured with actual receivers deployed for research purposes provide additional evidence on practical tracking performance, loop convergence, and the reliability of navigation-message decoding [6, 7].

Complementing academic studies, Capua and Bottaro [8] report on a GNSS software-receiver framework designed for governmental and mission-critical applications emphasising the importance of maintaining tracking accuracy under adverse situations such as weak signals, multipath, and interference. Their work focuses on the implementation strategies that preserve stability under these conditions; they highlight how a robust receiver design remains essential for ensuring secure and dependable navigation services.

J. Lohan et al. [9] represent a comprehensive discussion on methods for the acquisition and tracking of GNSS signals, emphasising the Galileo system. The goal is to promote the robustness and accuracy of acquisition and tracking techniques, with new algorithms specifically intended to perform well in dynamic scenarios and adverse signal conditions. The paper dwells on the different tracking loops and approaches and how they contribute to enhance the overall performance in GNSS receivers.

S. Naveen Pitchumani et al. [10] provides the mathematical modelling for an IRNSS receiver. The authors give a detailed explanation about the IRNSS receiver aspects along with mathematical support that helps a researcher willing

to work on IRNSS receiver. Chittimalla Srinu and Laxminarayana Parayitam [11] evaluate the performance metrics of a GNSS-SDR for receiving and processing L5 IRNSS signals using an economical RF front-end. They focused on the tracking capability of the SDR receiver in processing L5 signals and illustrate how various tracking algorithms influence the quality of the positioning estimates. The paper investigates the trade-offs between receiver cost and performance, illustrating that even low-cost receivers can provide acceptable performance if suitable tracking techniques are employed.

Dinesh L Mute and Susmita Bhattacharyya [12] propose the capability of processing signals of both GPS and NavIC constellations. The authors highlight the enhancement in the robustness of the tracking loop to maintain signal integrity from multipath effects, interference, and other adversarial conditions. A hybrid approach to tracking by combining various loop types is presented to improve tracking of the signal under different conditions, thus making the overall position accuracy better.

Hiep Van Hoang et al. [13] performed the field experiments in Hanoi, Vietnam, a location situated at the fringe of NavIC's primary service area to analyse the positioning service at Vietnam using IRNSS. As IRNSS-SPS signal characteristics are similar to those of GPS L1 C/A, the authors have reused the acquisition and tracking blocks of the Matlab GPS SDR with some minor modifications. The acquisition module is redesigned using a lightweight convolutional neural-network (CNN) to classify delay–Doppler patches of the cross-ambiguity function that increases detection sensitivity by approximately 4dB compared to the classical FFT-based search. It provides a pathway to implement tracking algorithm using CNN for which a strong basic knowledge of tracking is needed.

Mohanty A and Gao G [14] have done an extensive survey and have explored the application of ML methods for GNSS based positioning, highlighting the potential areas for future research and development in ML-based GNSS positioning. The thorough understanding of tracking algorithm helps to apply the ML algorithms for tracking process. Further, in [15] the authors Bhardwajan et al., detailed the design considerations and the architecture of a Software SDR capable of processing the new NavIC L1-SPS signals provided by the newest satellite of NavIC constellation- NVS-01. The thorough understanding of tracking of L5 signal helps to implement the tracking for L1-SPS signal. K Guddad and K L Sudha [16] represented the various acquisition techniques and compared the results that are used in the current paper to implement tracking algorithm using real IRNSS signals. Typical GNSS receiver performance depends on the carrier-to-noise density ratio (C/N_0). Acquisition generally requires $C/N_0 > 28–30$ dB-Hz, while stable carrier tracking is achieved above 30 dB-Hz. Reliable navigation data demodulation typically requires $C/N_0 > 33–35$ dB-Hz, and high-quality measurements are obtained for $C/N_0 > 40$ dB-Hz. These thresholds are approximate and depend on receiver design, integration time, loop bandwidth, and signal conditions. Stable tracking is typically achieved above 30 dB-Hz [2, 17, 18].

Hence, the tracking algorithm is the main thing to improve the reliability and accuracy of GNSS systems, such as GPS, NavIC and multi constellation systems. It overcomes the limitations created by signal interference and degradation and provides robust and uninterrupted tracking under real-world conditions which directly impacts navigation through complicated environments, such as urban canyons or heavily constructed areas, where conventional tracking will be difficult. A thorough grasp of GNSS tracking necessitates knowledge of the Costas loop, second-order PLL behavior, and the application of PLLs in DLL or Frequency Locked Loop (FLL) topologies. This paper reviews these fundamental concepts and presents corresponding results obtained using real IF data recorded from an IRNSS User Receiver. The work aims to provide a clear and practical reference for researchers and practitioners working on GNSS/IRNSS receiver design through mathematical analysis of the tracking process and step by step implementation of the same using real IF data captured by a real IRNSS receiver installed in IRNSS Laboratory of Jain University. Implemented tracking loop's performance is analysed using parameters such as frequency and phase jitter and the results show that the tracking loop is stable.

3. GNSS Receiver Methodology

A typical scheme for demodulating the received signal is illustrated in Fig. 1. In this process, a locally generated carrier at the appropriate sampling frequency is first multiplied with the incoming signal to remove the carrier modulation applied at the transmitter. Subsequently, the locally produced PRN code also sampled at the same rate is multiplied with the carrier-wiped signal to eliminate the DSSS spreading, thereby recovering the underlying navigation message. The received signal is processed step-by-step during the two primary stages: acquisition and tracking to remove carrier and code modulation.

In the acquisition stage, the receiver correlates the incoming waveform with the internally generated replicas of both carrier and PRN code [16]. Through this comparison, the system obtains the rough estimates of the signal's code phase and its Doppler-shifted carrier frequency as initial values which provide a practical starting point for the subsequent tracking operations. The receiver gradually sharpens these early estimates, adjusting them until the modulation imposed by the transmitter is effectively undone in the tracking module.

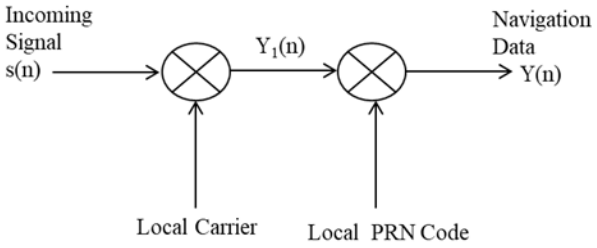


Fig. 1. Typical GNSS signal demodulation scheme.

In any GNSS receiver the primary task of the tracking phase is to generate the replicas of the carrier and the PRN code locally at the receiver to match the transmitted waveform as closely as possible. When this alignment is maintained, the receiver is able to remain locked onto a particular satellite and recover the navigation data embedded in the signal [17, 18]. Achieving such alignment is a dynamic process in which the receiver must continuously correct for Doppler shifts and changes in code phase that arise due to the relative motion between the user and the satellite. These adjustments feed directly into the quality of the demodulated measurements, which means that the stability and fidelity of the tracking process are highly tied to the receiver's positioning accuracy. Over time, researchers have proposed numerous tracking strategies aimed at improving performance under challenging conditions. Many of these approaches focus on mitigating the effects of noise, signal fading, and other environmental factors that can compromise loop stability. As GNSS applications increasingly demand reliability, particularly in domains such as autonomous navigation and aerospace systems, the receiver's ability to sustain accurate and consistent tracking has become even more critical [19].

3.1. IRNSS Signal

IRNSS satellites use a PRN sequence C(t) to first distribute navigational data D(t), which is then used to modulate the L5 carrier along with S-band carrier signal using BPSK modulation to create the combined navigation signal which is sent to the user. For simplicity of representation considering only L5 signal, the signal transmitted from the k^{th} satellite $S_{kT}(t)$ (T- indicating the transmitted signal), using BPSK modulation with f_{L5} - the frequency of IRNSS-L5 carrier signal transmitted from satellite, $C_k(t)$ - the PRN code sequence, $D_k(t)$ - the navigation data sequence and P_C - the power of PRN code, is represented by (1).

$$S_{kT}(t) = \sqrt{2P_C}C_k(t)D_k(t)\cos(2\pi f_{L5}t) \tag{1}$$

The received signal $S_R(t)$, (R- indicating received signal) at the receiver front end is given by (2).

$$S_R(t) = \sqrt{2P_C}C_k(t)D_k(t)\cos(2\pi f_{L5}t) + N(t) \tag{2}$$

where $N(t)$ is the noise added during the transmission.

The signal $S_{RIF}(t)$, after filtering and down-conversion to the intermediate frequency (IF), is expressed as in (3).

$$S_{RIF}(t) = A_cC_k(t)\,D_k(t)\cos(2\pi f_{IF}t) \tag{3}$$

where A_c is the amplitude of signal after filtering and down conversion; f_{IF} - the carrier frequency after down conversion to IF and k indicates the satellite number. Upon digitization of $S_{RIF}(t)$ using an Analog to Digital Converter with sampling frequency fs, the discrete-time signal $S_R(n)$can be represented as in (4)

$$S_R(n) = A_cC_k(n)\,D_k(n)\cos(\frac{2\pi f_{IF}}{fs}n) \tag{4}$$

The navigation data $D_k(n)$ can be separated by multiplying the digitised received signal $S_R(n)$ with locally produced replicas of the PRN code and carrier having the appropriate sampling frequency. When the locally produced carrier is perfectly aligned with the incoming signal in terms of both frequency and phase, the correlation process yields the output $y_1(n)$.

$$\begin{aligned} y_1(n) &= S_R(n)\cos\left(\frac{2\pi f_{IF}}{fs}n\right) \\ &= [A_cC_k(n)\,D_k(n)\cos(\tfrac{2\pi f_{IF}}{fs}n)\,]\cos(\tfrac{2\pi f_{IF}}{fs}n) \end{aligned}$$

$$= \frac{A_c C_k(n) D_k(n)}{2}\left[1+\cos\left(\frac{4\pi f_{IF}}{fs}n\right)\right]$$
$$= \frac{A_c C_k(n) D_k(n)}{2} + \frac{A_c C_k(n) D_k(n)}{2}\cos\left(\frac{4\pi f_{IF}}{fs}n\right) \quad (5)$$

The high-frequency carrier term in (5) is suppressed through low-pass filtering, resulting in the data sequence combined with the code $C_k(n)$. The LP filter output is given in (6).

$$y_{1_{LP}}(n) = \frac{A_c C_k(n) D_k(n)}{2} \quad (6)$$

The code $C_k(n)$ is then removed by correlating $y_{1_{LP}}(n)$ with a locally produced code replica. The correlator output $y(n)$ provided in (7) yields the scaled navigation data when the locally produced replica exactly matches the code in the received signal.

$$y(n) = \sum_{n=0}^{N-1} C_k(n) C_k(n) D_k(n) \; = N D_k(n) \quad (7)$$

Here, N represents the length of the correlation interval. The receiver must produce carrier and code replicas that closely match the incoming signal in order to sustain dependable signal processing, which necessitates constant modifications to the predicted carrier frequency and code phase. A PLL is used to accomplish this ongoing refinement [20].

3.2. Second order PLL

When building GPS or GNSS receivers, researchers typically favor a second-order PLL, particularly for carrier and code tracking. The reason is when the signal frequency varies abruptly or gradually over time, a first-order loop with a single integrator, tends to leave behind residual errors since it is simply not robust enough [21]. In GPS systems, a Delay Lock Loop (DLL) carries out the code tracking by replicating the PRN sequence, while a Costas loop typically handles the carrier tracking, generating an accurate carrier estimate. Reliable tracking performance is achieved when the same configuration is applied to IRNSS signals too.

A first-order loop filter and a phase discriminator, together with a Voltage-Controlled Oscillator (VCO) constitute a second-order PLL. Fig. 2(a) and Fig. 2(b) illustrate the analog and digital implementations of a typical linearized second-order PLL respectively.

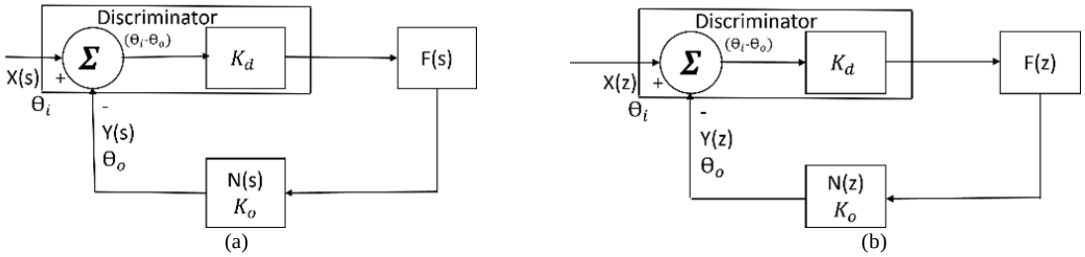


Fig. 2. Second order Linearized PLL models (a) Analog version (b) Digital version.

The analog transfer function of first order filter is provided in (8).

$$H(s) = \frac{K_d F(s) N(s)}{1 + K_d F(s) N(s)} = \frac{2\zeta\omega_n s + {\omega_n}^2}{s^2 + 2\zeta\omega_n s + {\omega_n}^2} \quad (8)$$

where $F(s) = \frac{1+\tau_2 s}{\tau_1 s}$ and $N(s) = \frac{K_o}{s}$; K_o and K_d are gains of the VCO and discriminator respectively; τ_1 and τ_2 are filter parameters that depend on loop gain $K_o K_d$; $\omega_n = \sqrt{\frac{K_o K_d}{\tau_1}}$ represents the natural frequency; and $\zeta = \frac{\tau_2 \omega_n}{2}$ represents damping ratio.

The digital transfer function of the PLL model $H_1(z)$ is given by (9) with T being the sampling interval of 1ms.

$$H_1(z) = \frac{(4\zeta\omega_n T + (\omega_n T)^2) + 2(\omega_n T)^2 z^{-1} + ((\omega_n T)^2 - 4\zeta\omega_n T) z^{-2}}{(4 + 4\zeta\omega_n T + (\omega_n T)^2) + (2(\omega_n T)^2 - 8) z^{-1} + (4 - 4\zeta\omega_n T + (\omega_n T)^2) z^{-2}} \quad (9)$$

Fig. 3 illustrates the loop filter of digital PLL and the digital transfer function $H_2(z)$ is represented in (10), which can be obtained by using $F(z) = \frac{(C_1 + C_2) - C_1 z^{-1}}{1 - z^{-1}}$ and $N(z) = \frac{K_o z^{-1}}{1 - z^{-1}}$ in $H_2(z) = \frac{\theta_o(z)}{\theta_i(z)} = \frac{K_o F(z) N(z)}{1 + K_d F(z) N(z)}$

$$H_2(z) = \frac{K_o K_d (C_1+C_2) z^{-1} - K_o K_d C_1 z^{-2}}{1+(K_o K_d (C_1+C_2)-2) z^{-1} + (1-K_o K_d C_1) z^{-2}} \quad (10)$$

where C1 and C2 are coefficients given by (11) and (12).

$$C_1 = \frac{8\zeta\omega_n T}{K_o K_d((\omega_n T)^2 + 4\zeta\omega_n T + 4)} \quad (11)$$

$$C_2 = \frac{4(\omega_n T)^2}{K_o K_d((\omega_n T)^2 + 4\zeta\omega_n T + 4)} \quad (12)$$

The natural frequency $\omega_n$and the noise bandwidth B_L are given by, $\omega_n = \frac{8\zeta B_L}{1+4\zeta^2}$ and $B_L = \frac{\omega_n(\zeta+\frac{1}{4\zeta})}{2}$

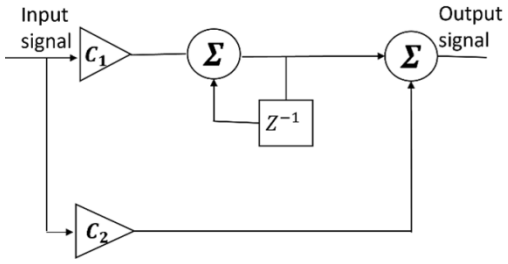


Fig. 3. The loop filter of second order digital PLL.

The damping ratio (ζ) and noise bandwidth (B_L) are signal-dependent parameters that significantly influence tracking-loop performance. The value of ζ governs both the settling time and overshoot of the loop response; therefore, its selection is a trade-off between rapid convergence and stability. Prior studies indicate that ζ = 0.7 provides an effective balance and is widely used in GNSS tracking applications. The noise bandwidth B_L also plays a crucial role by determining the loop's convergence rate and the amount of noise admitted into the system. Higher B_L results in faster lock but increases post-lock noise, while a lower B_L reduces noise at the expense of slower acquisition. Typical GNSS receivers use DLL bandwidth in the range of 1Hz–2 Hz for Low noise and high accuracy, and a PLL bandwidth in the range 15Hz –25Hz for stability and Doppler tracking. Also keeping a ratio of 10:1 between PLL and DLL bandwidth ensures stable carrier-aided code tracking, which is essential for reliable receiver operation [14, 15, 18]. Hence B_L = 2Hz for code tracking and B_L= 20Hz for carrier tracking are chosen in this work.

For ζ = 0.7, the natural frequencies computed are ω_n= 2Hz (code loop), ω_n= 20Hz (carrier loop). For the IRNSS data considered in this work the values of the loop-filter coefficients C_1 and C_2 are obtained as C_1=0.051588120220523, C_2=0.001394273519474 for carrier tracking loop, and C_1=0.005283284821870, C_2=$1.427914816721669\times10^{-5}$ for code tracking loop with $K_o K_d$ =1, ζ = 0.7, B_L=2Hz for code tracking and 20Hz for carrier tracking. The resulting tracking performance using these parameters is presented in the Results section.

3.3. Carrier tracking

The acquisition stage provides the initial carrier frequency to the tracking stage, which typically contains an error of several tens of hertz. The tracking loop, implemented using a PLL or FLL with a second order loop filter as shown in Fig. 4, continuously refines this estimate to generate an accurate replica of the carrier needed to cancel carrier modulation from the received signal. The loop guides the local carrier generator towards the actual satellite carrier frequency by gradually improving both the frequency and phase as the tracking operation progresses. Predefined lock criteria, which outline the maximum amount of frequency inaccuracy that can be accepted, are followed by this adjustment. Once the loop settles the carrier is precisely in line with the received signal and the receiver can successfully recover the navigation data [21].

As shown in Fig. 4 the carrier component is removed by the carrier-loop discriminator and loop filter working together. After being filtered, the phase error between the incoming signal and the locally generated carrier is produced by the loop discriminator and given back to the numerically controlled oscillator (NCO), which modifies the frequency of the local carrier. As the conventional PLL is highly sensitive to bit transitions in the navigation data (i.e. 180 °phase reversals), a Costas loop is employed for carrier tracking.

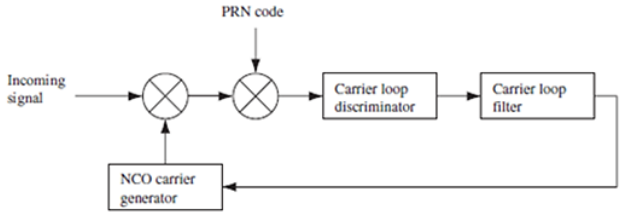


Fig. 4. Block diagram of a basic tracking loop.

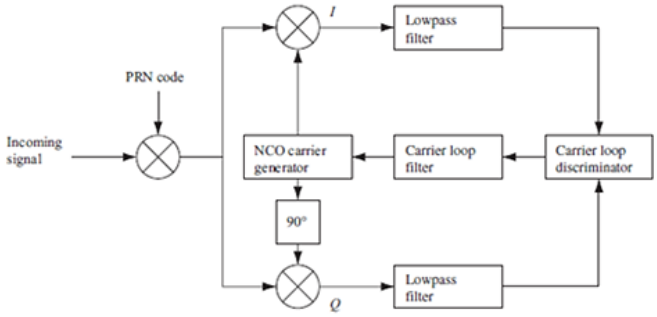


Fig. 5. Costas loop for carrier tracking.

Fig.5 illustrates the operation of the Costas loop. In this architecture, locally produced PRN code is first multiplied by the incoming signal. The in-phase (I) and 90-degree phase-shifted (Q) copies of the locally generated carrier are then combined with the resultant signal to provide I and Q channel outputs, respectively. Any phase offset that remains after the PRN code and the received signal are properly matched indicates the phase difference between the incoming carrier and the local carrier. Accordingly, I and Q outputs contain constituents related to this phase difference. After low-pass filtering, the higher-frequency terms are removed, leaving only the terms that reflect the true phase relationship amongst the received and locally generated carriers as given by (13) and (14).

$$I^{k}(n) = D^{k}(n)\cos(\omega_{IF}n)\ \cos(\omega_{IF}n + \phi) = \frac{D^{k}(n)}{2}\cos(\phi) + \frac{D^{k}(n)}{2}\cos(2\omega_{IF}n + \phi) \tag{13}$$

$$Q^{k}(n) = D^{k}(n)\ \cos(\omega_{IF}n)\ \sin(\omega_{IF}n + \phi) = \frac{D^{k}(n)}{2}\sin(\phi) + \frac{D^{k}(n)}{2}\sin(2\omega_{IF}n + \phi) \tag{14}$$

where k is satellite number. The higher order terms in (13) and (14) of $I^{k}(n)$ and $Q^{k}(n)$ are removed by utilizing a low pass filter resulting in I^{k} and Q^{k}; where $I^{k} = \frac{D^{k}(n)}{2}\cos(\phi)$, $Q^{k} = \frac{D^{k}(n)}{2}\sin(\phi)$ i.e. I component is related to the cosine of the phase error, while the Q component is related to the sine of the phase error. The phase angle of the resulting complex signal $x^{k} = I^{k} + j\,Q^{k}$ gives the phase error φ_e between input and local carrier as given by (15). The ratio of the Q to I output provides a direct measure of the phase error (φ_e), which is obtained through an arctangent operation.

$$\frac{I^{k}}{Q^{k}} = \tan(\varphi_e) \text{ or } \varphi_e = \tan^{-1}\left(\frac{I^{k}}{Q^{k}}\right) \tag{15}$$

In general, the phase error is written as $\varphi_e = k_d \tan^{-1}\left(\frac{Q^{k}}{I^{k}}\right)$, where k_d is the gain of the discriminator. The discriminator described above is known as arctan discriminator. The Costas loop discriminator uses this phase error as its input. Since it can provide precise phase error estimates, the arctangent discriminator, a crucial aspect of the Costas loop, is highly regarded for its accuracy, especially in low Signal to Noise Ratio (SNR). Even though it requires more computing power than more straightforward discriminators, the trade-off is frequently beneficial in real-world scenarios. The resistance to 180-degree phase shifts, which usually result from navigation data bit transitions, is one of the main advantages of the Costas loop. These reversals are handled smoothly by the Costas loop, which keeps carrier tracking steady without losing lock. Since it provides both strong phase stability and dependable data demodulation, it continues to be the preferred design for carrier tracking in the majority of GNSS receivers.

3.4. Code Tracking

The receiver must make sure that the phase of the locally produced PRN sequence closely matches the phase of the code in the received signal in order to successfully eliminate the PRN code modulation from the incoming signal. This fine alignment is taken care of during the code-tracking stage, where a DLL incrementally improves the crude code-phase estimate that was received after acquisition. In order to do this, the DLL compares the arriving signal with the copies of three significantly shifted versions of the local PRN code, each half a chip apart known as early, prompt and late replicas. Fig. 6 and Fig. 7 illustrate this configuration, which enables the loop to identify and rectify even minute phase misalignments. Since one replica is advanced by half a chip ("early") and another is delayed by half a chip ("late"), this configuration is commonly referred to as an early–late tracking loop.

In the implementation shown in Fig. 6 the carrier component is first removed by multiplying the received signal with the carrier produced locally, that is already aligned through the carrier-tracking loop. The resulting baseband signal is then compared using correlation operation with the three PRN replicas—early (E), prompt (P), and late (L) producing three corresponding outputs. These correlation outputs form the basis for estimating the code-phase error and adjusting the local code generator to retain precise synchronization between the received and locally produced PRN sequences.

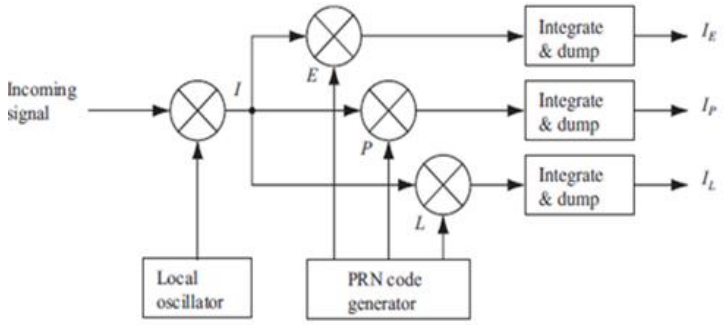


Fig. 6. Basic code tracking loop.

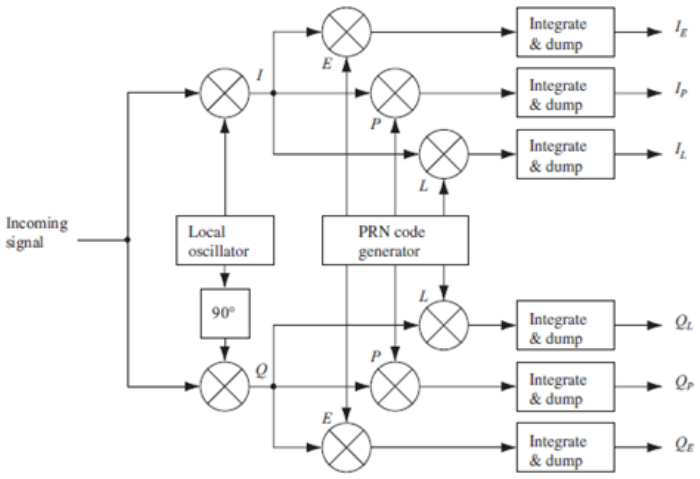


Fig. 7. Code tracking loop with six correlators.

The integrate-and-dump block accumulates the correlation products over a 1ms interval and produces the Early, Prompt, and Late outputs (I_E, I_P and I_L) as shown in Fig. 6 and Fig. 7. These values show how well each locally created code matches the code present in the received signal. The code phase is adjusted according to the correlator with the highest output. For instance, Fig. 8(a) shows the "Late" correlator peak, indicating that the local code is behind and must be advanced by half a chip. Further, Fig. 8(b) shows a maximum at the "Prompt" correlator, indicating correct alignment, whereas in Fig. 8(c) the "Early" correlator peak indicates that a half chip delay must be introduced in the local code for perfect match.

Under ideal conditions when the local carrier is fully aligned with frequency and phase, a three-correlator DLL, such as that in Fig. 6 is sufficient. In practical, real-time conditions, small residual phase errors are almost unavoidable. To address these, the six-correlator DLL configuration shown in Fig. 7 is commonly used. This design splits the signal into two parallel processing paths: an in-phase (I) branch driven by the locally produced carrier, and a quadrature (Q) branch that uses the same carrier shifted by 90 degrees. When the carrier loop is properly locked then the major part of the signal energy appears in the I-branch, as depicted in Fig. 9.

However, if there is any phase offset between the arriving signal and the locally produced carrier, some of the signal energy shifts into the Q-branch, as shown in Fig. 10. The tracking loop maintains accurate code tracking by compensating for this phase mismatch by monitoring and merging data from both I and Q arms.

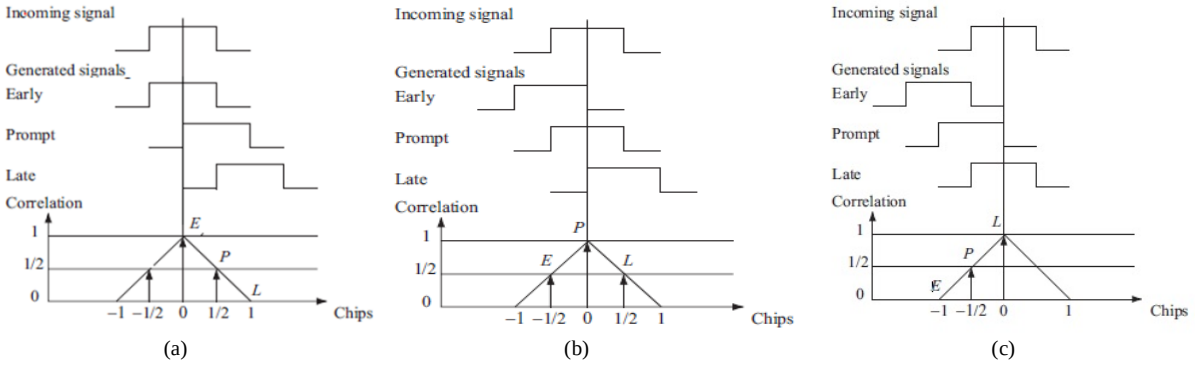


Fig. 8. Early-Late correlator showing maxima at (a) early, (b) prompt, & (c) late replicas [9].

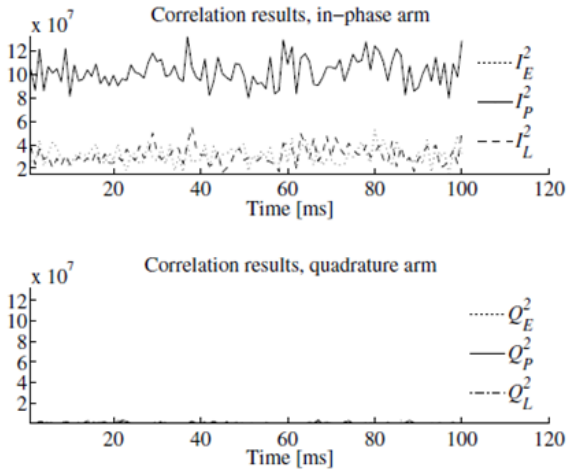


Fig. 9. Six-correlator output under perfect alignment.

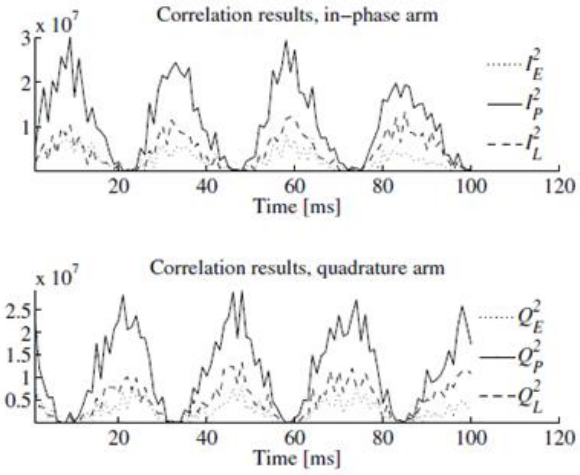


Fig. 10. Energy distribution caused by carrier phase error in the I and Q arms of a six-correlator.

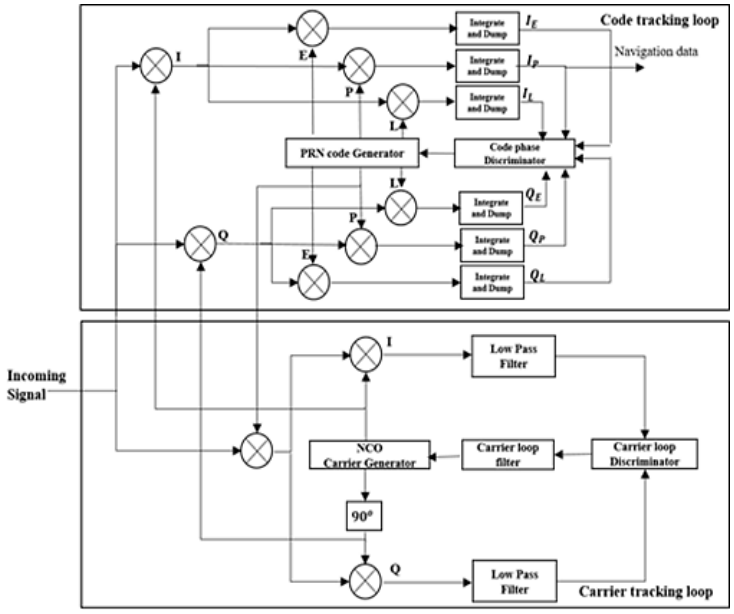


Fig. 11. DLL and PLL combined for carrier and code tracking.

The distance between the Early, Prompt, and Late correlator outputs is an important design parameter in a DLL as it directly affects the noise bandwidth of the loop. The DLL becomes more resilient to fast signal dynamics and increased noise levels when the Early–Late spacing is comparatively large, usually more than half a chip, which reduces the likelihood that it will lose lock in difficult circumstances [22,23]. Conversely, a smaller spacing increases the code-phase estimate's accuracy but increases the loop's susceptibility to noise and sudden changes in the signal. Many contemporary GNSS receivers use discriminators that enable the Early-Late spacing to change in real time in order to balance these conflicting requirements making the receiver robust which helps the receiver to respond more effectively to sudden changes in SNR, enhancing overall robustness, especially in situations involving high user motion or intermittent signal blockage.

Among three discriminators viz., Early minus Late power discriminator, the dot-product discriminator and the normalized Early minus Late power discriminator, the normalized version is frequently preferred as it uses data from both the in-phase and quadrature components making its performance partially independent of the carrier tracking loop. Additionally, the normalization step stabilizes the discriminator output over a broad range of signal amplitudes and SNR values — a useful advantage considering that GNSS signals often undergo notable and unanticipated strength variations during real-world operation.

The discriminator functions of the three discriminators mentioned are given by D_{EL}, D_{DOT} and D_{NORM} in (16a), (16b), & (16c)

$$D_{EL} = (I_E^2 + Q_E^2) - (I_L^2 + Q_L^2) \tag{16a}$$

$$D_{DOT} = I_P(I_E - I_L) + Q_P(Q_E - Q_L) \tag{16b}$$

$$D_{NORM} = \frac{(I_E^2 + Q_E^2) - (I_L^2 + Q_L^2)}{(I_E^2 + Q_E^2) + (I_L^2 + Q_L^2)} \tag{16c}$$

Fig. 11 shows the combined code and carrier tracking structure. The carrier tracking loop is depicted in the lower section, while the code tracking loop is shown in the upper section. The output of the PRN code generator in this configuration flows into the carrier loop's first multiplier. This process completely removes the code modulation from the incoming signal after the loop latches onto the signal, enabling precise tracking of the carrier component. Likewise, the output of the NCO-based carrier generator feeds the first multiplier in the code tracking loop, and when this loop is locked, it effectively removes the carrier component. When both the code and carrier loops are successfully locked, the system outputs the navigation data bits with minimal noise, as demonstrated in Fig.15(c) in the results section.

The performance of the tracking loop can be measured using parameters such as phase jitter (σ_φ) and frequency jitter (σ_f) which are obtained from the phase error of the correlator using (17) and (18), T being the integration time.

$$\sigma_\varphi = std(\phi_e) \tag{17}$$

$$\sigma_f = \frac{\sigma_\varphi}{2\pi T} \tag{18}$$

4. Results and Discussion

The tracking algorithm is implemented in MATLAB using real IF data recorded from the IRNSS-UR, a research-oriented IRNSS user receiver installed at the IRNSS laboratory of Jain University, Bengaluru. The receiver samples the IF signal at 16.221 MHz, with an overall system sampling rate of 56 MHz, resulting in 56,000 samples per 1ms interval. A correlator spacing of ±½ chip is employed for the tracking tests. The local carrier replicas are generated at the same sampling frequency as the receiver i.e. 56 MHz sampling rate. For analysis and plotting, a representative portion of the 1ms data segment is used.

Table 1. The tracking types and parameter values.

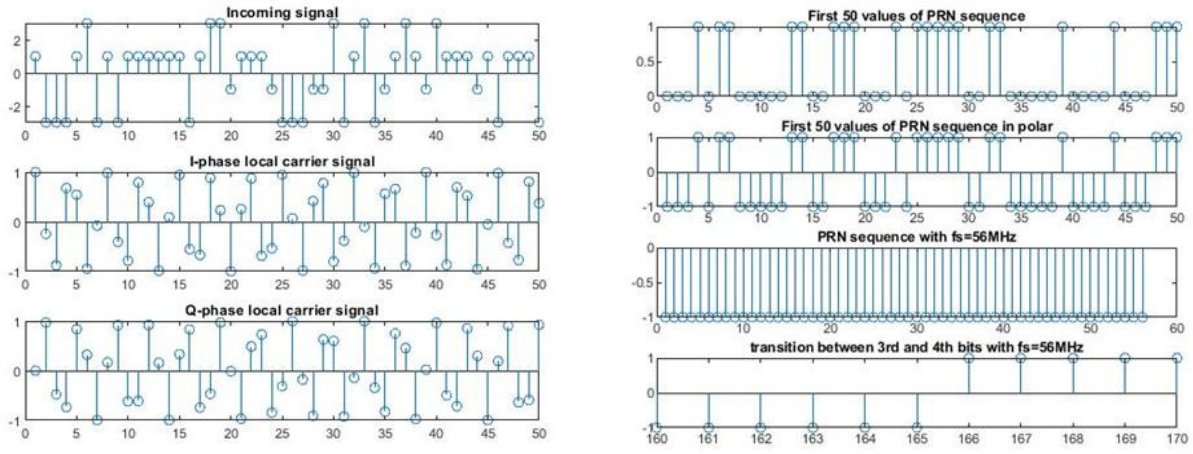
Tracking type	Loop Gain ($K_o K_d$)	Damping ratio (ζ)	Noise Bandwidth (B_L)
Code Tracking	1	0.7	2
Carrier Tracking	1	0.7	20

Table 2. The performance parameters of the designed tracking loop.

Metric	Value	Description
Phase jitter (σ_φ)	0.0347 rad	RMS phase error after removing DC bias
Phase jitter (degrees)	1.986 °	Indicates very stable PLL lock
Frequency jitter (σ_f)	5.516908 Hz	Computed from $\sigma_\varphi/(2\pi T)$, T = 1ms
Frequency jitter (derivative method)	5.524187 Hz	From derivative of unwrapped phase
Estimated C/N₀	42.21 dB-Hz	Using loop bandwidth Bn = 20 Hz
Coherent integration time (T)	1 ms	PLL update rate

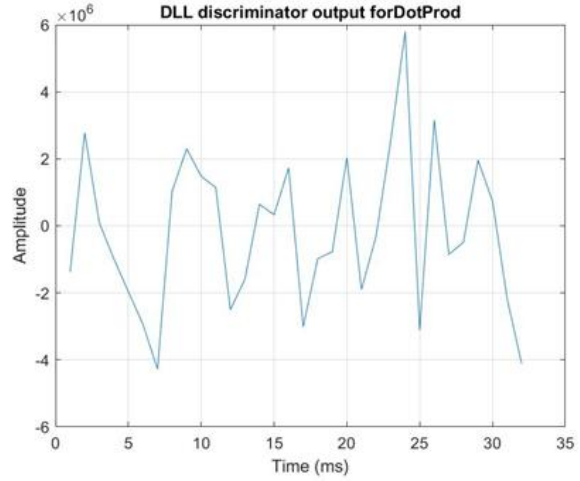
Fig. 12(a) and Fig. 12(b) illustrate the portions of the received data, local carrier replicas, and PRN sequences used during the tracking process. Based on the earlier discussion, the loop gain, the damping ratio, and the noise band-width values selected for carrier tracking are summarized in Table 1, and the corresponding results are presented in Fig. 13, Fig. 14, and Fig. 15. All carrier-tracking loop parameters are identical to those used for code tracking, except for the noise bandwidth. Tracking is performed on 1024ms of data, and the code tracking loop is configured to lock either when the phase error falls within ±0.0005 or after 1000 iterations—whichever occurs first. Both tracking loops operate over the full 1024ms data interval.

Fig. 13 shows a segment of the discriminator outputs for the three non-coherent DLL discriminators. Further, the normalized Early minus Late discriminator in Fig. 13(c) varies within a fixed range between +1 and –1, unlike the larger unbounded values observed in Fig. 13(a) and Fig. 13(b). This normalized behavior makes it particularly suitable for signals with varying SNRs or fluctuating power levels.

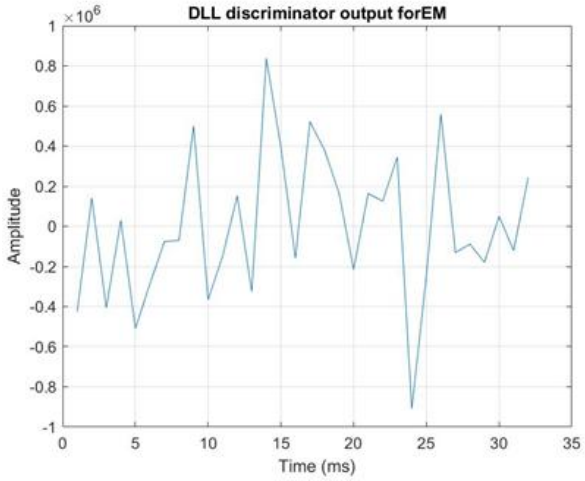


(a) (b)

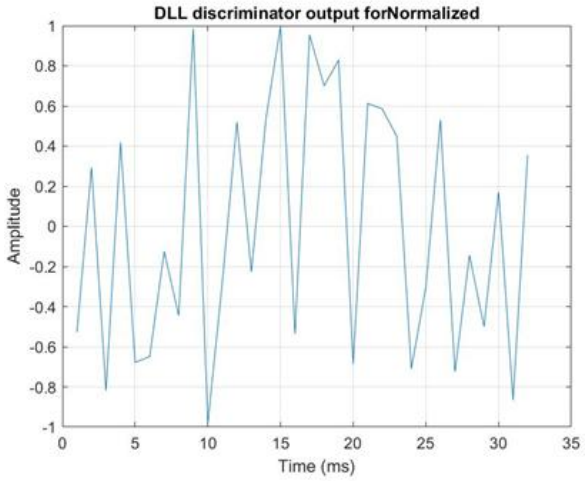
Fig. 12. Waveform plot of (a) Incoming signal and local carrier & (b) PRN sequence in various stages.



(a)



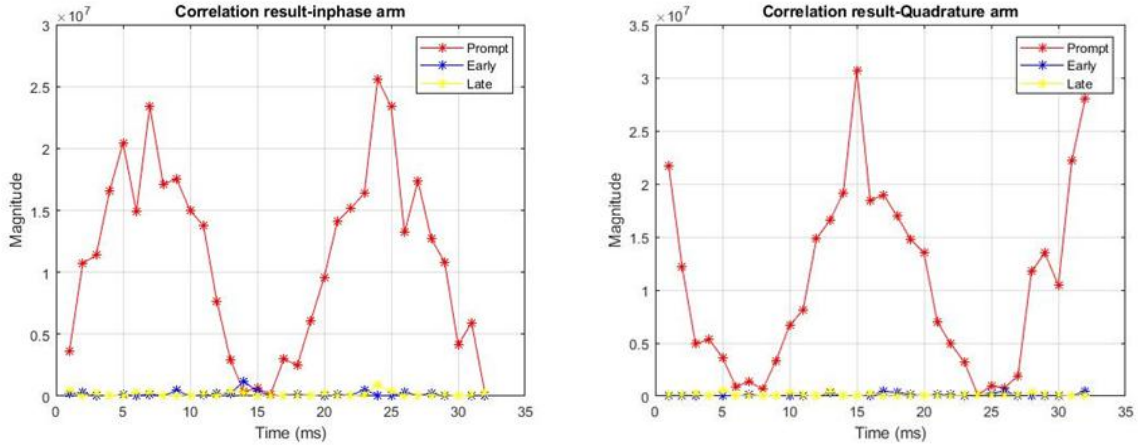
(b)



(c)

Fig. 13. DLL discriminator outputs of (a) Dot product (b) Early-Late & (c) Normalized.

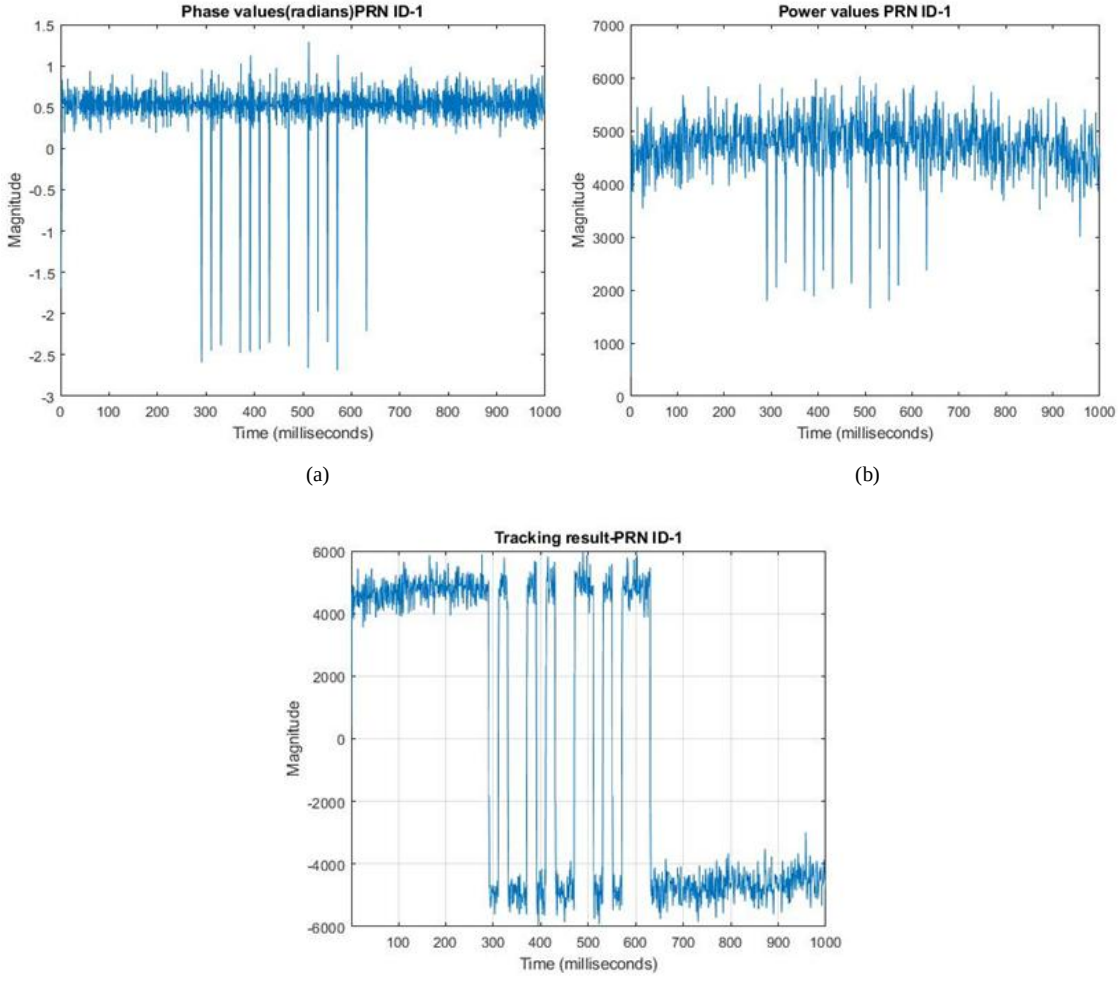
Further, Fig. 14(a), and Fig. 14(b) display portions of the in-phase (I-arm) and quadrature (Q-arm) outputs from all the six correlators by illustrating how the signal energy is distributed across them. The energy in the Early and Late correlators indicates the degree of code-phase misalignment between the received and locally created codes, whereas the prompt correlator has the highest energy.



(a) (b)

Fig. 14. Correlation result of (a) an in-phase arm (b) quadrature arm.

Furthermore, Fig. 15 presents the tracking results obtained using the normalized discriminator for code and carrier tracking with the Costas loop over the 1024ms data for Satellite 1.



(a) (b)

(c)

Fig. 15. Tracking results with (a) Phase values (b) Power values & (c) Navigation bits.

Carrier tracking loop performance metrics derived from the prompt correlator outputs of the IRNSS L5 signal are shown in Fig. 16 and tabulated in Table 2. Fig. 16(a) shows the phase error time series using 1-ms coherent integration where the phase error varies between ±0.3 radians. Fig. 16(b) depicts the histogram of phase error showing an RMS jitter of 0.0347 rad (1.986 °). Fig. 16(c) shows instantaneous frequency error obtained from the derivative of the

unwrapped phase, indicating an RMS frequency jitter of approximately 5.52 Hz. Since direct C/N₀ measurements were not available, under the assumption of thermal-noise-dominated tracking, an effective carrier-to-noise density C/N_o is back-estimated from the PLL phase jitter using the relationship $\sigma_\phi^2 \approx \frac{B_n}{C/N_o}$, giving $C/N_o \approx \frac{B_n}{\sigma_\phi^2}$. The back estimated value is approximately 42.2dB-Hz with a loop noise bandwidth of 20Hz confirming stable carrier tracking.

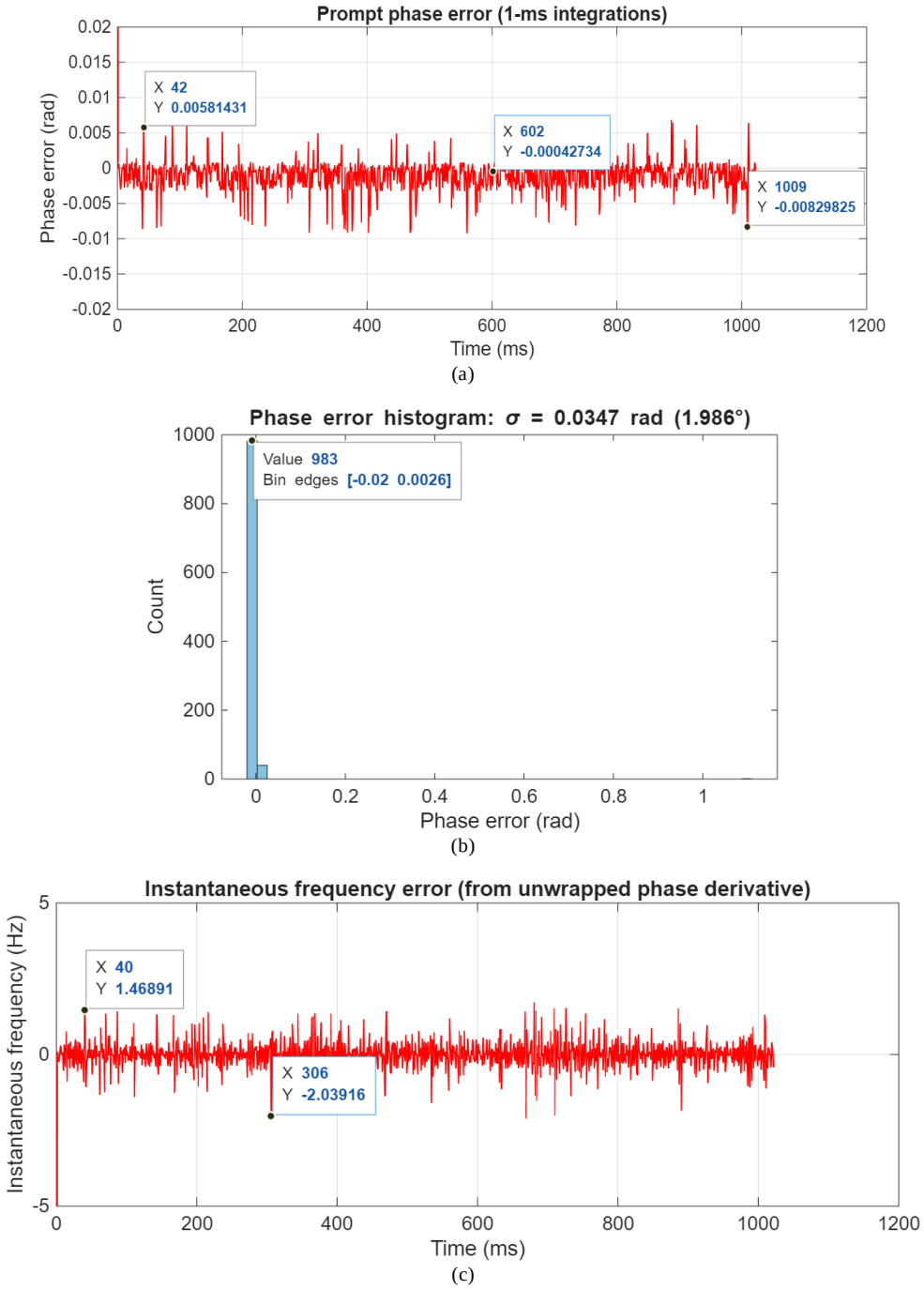


Fig. 16. Carrier tracking loop performance metrics derived from the prompt correlator outputs of the IRNSS L5 signal. (a) Phase error time series using 1-ms coherent integration. (b) Histogram of phase error (c) Instantaneous frequency error obtained from the derivative of the unwrapped phase.

5. Conclusion

The IRNSS satellites are tracked successfully for the signal received from an open sky antenna using a similar concept and parameters used for GPS with suitable changes for IRNSS data. The navigation bits are recovered successfully for 1024ms. The performance parameters show that the designed loop filter is stable and can be used to process the open sky IRNSS signals. This work uniquely details the tracking process along with supporting mathematical background using real IF data taken from real hardware and hence it is very beneficial for the researchers

in guiding through the course of GNSS/IRNSS signal tracking right from the basic concept till the navigation bit stream extraction using IRNSS data, which is a very basic need while designing or analyzing the GNSS/IRNSS receivers. Further work can be done on decoding the data and position finding. The work may also be extended for the signals acquired in an indoor scenario and analysed using similar techniques for GPS to study the effect of obstacles on received signals.

All the Declarations and Statements

Author Contributions Statement
All authors have equal contribution.

All authors have read and agreed to the published version of the manuscript.

Conflict of Interest Statement
The authors declare no conflict of interest.

Funding Declaration
Not Applicable.

Data Availability Statement
Not Applicable.

Ethical Declarations
Not Applicable.

Acknowledgments
Authors sincerely appreciate ISRO, Jain University and Dr. Raju Garudachar from Jain University for providing the data with necessary details. Further, Authors would like to express their gratitude to the reviewers for their recommendations that improved the presentation.

Declaration of Generative AI in Scholarly Writing
Not Applicable.

Abbreviations
The following abbreviations are used in this manuscript:

CNN - Convolutional Neural Network
DLL - Delay Lock Loop
DSSS - Direct Sequence Spread Spectrum
FFT - Fast Fourier Transform
FLL - Frequency Locked Loop
GNSS - Global Navigation Satellite System
GPS - Global Positioning System
IF - Intermediate Frequency
IRNSS - Indian Regional Navigation Satellite System
ISRO - Indian Space Research Organization
ML - Machine Learning
NCO - Numerically Controlled Oscillator
PLL - Phase-Locked Loop
PRN - Pseudo Random Noise
RMS - Root Mean Square
RNSS - Regional Navigation Satellite System
SDR - Software-Defined Radio
SPS - Standard Positioning Service
UR - User Receiver
VCO - Voltage-Controlled Oscillator

APPENDIX A/B/C…, with appendix title

Not Applicable.

References

[1] J. B.-Y. Tsui, Fundamentals of Global Positioning System Receivers. Hoboken, NJ, USA: John Wiley & Sons, 2000.

[2] J. J. Spilker Jr., P. Axelrad, B. W. Parkinson and P. Enge, Global Positioning System: Theory and Applications, vol. 1. Washington, DC, USA: AIAA, 1996.

[3] T. Pany et al., "GNSS Software-Defined Radio: History, Current Developments, and Standardization Efforts," Navigation, vol. 71, no. 1, article navi.628, Mar. 2024, doi: 10.33012/navi.628.

[4] S. Stevanović and B. Pervan, "A GPS Phase-Locked Loop Performance Metric Based on the Phase Discriminator Output," Sensors, vol. 18, no. 1, article 296, Jan. 2018, doi: 10.3390/s18010296.

[5] D. V. Fernandes, P. K. Jain, V. N. Srinivas, V. Chavan, K. M. Gayathri, and N. Thangadurai, "Acquisition and Tracking of S-Band Signals of Navigation with Indian Constellation (NavIC)," International Journal of Recent Technology and Engineering, vol. 8, no. 2, pp. 503–508, Jul. 2019. doi: 10.35940/ijrte.B1567.078219.

[6] M. T. R. Manjula and G. Raju, "Acquisition and Tracking of NavIC L5 Band Signals," Int. J. Appl. Eng. Res., vol. 12, no. 19, pp. 8115–8119, 2017.

[7] C. Srinu and L. Parayitam, "Performance Analysis of NavIC Software Receiver for Single Frequency Ionospheric Delay Corrections," in Proc. ION GNSS+ 2021, St. Louis, MO, USA, Sept. 2021, pp. 3886–3896, doi: 10.33012/2021.18059.

[8] R. Capua and A. Bottaro, "A GNSS Software Receiver for Governmental Applications," in Proc. ION GNSS 2011, Portland, OR, USA, Sept. 2011, pp. 813–823.

[9] J. Nurmi, E. S. Lohan, S. Sand, and H. Hurskainen, Eds., "GALILEO Positioning Technology," Signals and Communication Technology. Dordrecht, The Netherlands: Springer, 2015. doi: 10.1007/978-94-007-1830-2.

[10] S. N. Pitchumani, S. A. Sundar, T. Srinivasan and S. Savitri, "Mathematical Modelling of Indian Regional Navigation Satellite System Receiver," Defence Sci. J., vol. 67, no. 4, pp. 443–448, Jul. 2017, doi: 10.14429/dsj.67.11547.

[11] Chittimalla Srinu, Laxminarayana Parayitam, " Performance of GNSS-SDR for IRNSS L5 Signals Using a Low-Cost RF Front-End", NAVIGATION: Journal of the Institute of Navigation , June 2023, 70 (2) , navi.573, DOI: https://doi.org/10.33012/navi.573

[12] D. L. Mute and S. Bhattacharyya, "A Robust Signal Tracking Algorithm for GPS and NavIC Constellations," GPS Solutions, vol. 27, no. 3, Apr. 2023, doi: 10.1007/s10291-023-01444-2.

[13] Hiep Van Hoang , Ty Dinh Viet , Hung Pham Ngoc , Tung Hai Ta , Nguyen Dinh Thuan , "Performance Evaluation of a Deep Learning-Enhanced Software-Defined Receiver for IRNSS SPS Signals in Vietnam", 2025, Artificial Satellites, vol. 60, no. 4, pp. 137-160, DOI: 10.2478/arsa-2025-0008.

[14] Mohanty, A., & Gao, G. (2024). A survey of machine learning techniques for improving globalnavigation satellite systems. EURASIP Journal on Advances in Signal Processing, 2024(1), 73.https://doi.org/10.1186/s13634-024-01167-7.

[15] Bhardwajan, A.A., Dharmappa, D., Ganesh, T.S., Vashisth, S., Gupta, A.S. (2026). "Design Aspects of an SDR for the New NavIC L1 SPS Signals", Proceedings of Smart and AI Enabled Technology for Sustainable Development . SAIT 2023. Lecture Notes in Electrical Engineering, vol 1452. Springer, Singapore. https://doi.org/10.1007/978-981-96-9370-2_6.

[16] K. Guddad and K. L. Sudha, "Analysis of Acquisition Algorithms Using IRNSS Data," in Proc. CE2CT 2025, Bhimtal, Nainital, India, 2025, pp. 62–66, doi: 10.1109/CE2CT64011.2025.10939882.

[17] K. Borre, D. Akos, N. Bertelsen, P. Rinder and S. Jensen, A Software-Defined GPS and Galileo Receiver: A Single-Frequency Approach.New York, NY, USA: Springer, 2007, doi: 10.1007/978-0-8176-4540-3.

[18] P. Misra and P. Enge, Global Positioning System: Signals, Measurements, and Performance. Lincoln, MA, USA: Ganga-Jamuna Press, 2001.

[19] C. Macabiau, L. Ries, F. Bastide and J.-L. Issler, "GPS L5 Receiver Implementation Issues," in Proc. ION GPS/GNSS 2003, Portland, OR, USA, Sept. 2003, pp. 153–164. Available: http://www.ion.org/publications/abstract.cfm?articleID=5191

[20] Indian Space Research Organisation (ISRO), "Indian Regional Navigation Satellite System Signal-in-Space ICD for Standard Positioning Service," Version 1.1, ISRO-IRNSS-ICD-SPS-1.1, Aug. 2017.

[21] K. Krumvieda et al., "A Complete IF Software GPS Receiver: A Tutorial about the Details," in Proc. ION GPS 2001, Salt Lake City, UT, USA, Sept. 2001.

[22] J. H. Lee, D. W. Lim, J. H. Noh, G. H. Jo, C. Park, J. M. Ahn and S. J. Lee, "A GPS Multipath Mitigation Technique Using Correlators with Variable Chip Spacing," E3S Web Conf., vol. 94, 2019, Art. no. 03006, doi: 10.1051/e3sconf/20199403006.

[23] W. K. Khaing et al., "Analysis of Acquisition and Tracking Algorithms for Software GNSS Receivers," Int. J. Adv. Electron. Comput. Sci., vol. 2, no. 6, Jun. 2015.

Authors' Profiles



Kavita Guddad received her B. E degree in Electronics and Communication Engineering from Shri Taralabalu Jagadguru Institute of Technology (STJIT), Ranebennur under Karnataka University, Dharawad and M. Tech degree in Digital Communication and Networking from UBDT College of Engineering, Davangere. She is pursuing her Ph. D degree under the Department of Electronics and Communication Engineering, Dayananda Sagar College of Engineering, Bengaluru of Visvesvaraya Technological University, Belagavi. Currently she is working as Assistant Professor in the Department of Electronics and Communication Engineering, Dayananda Sagar College of Engineering, Bengaluru. She has more than 18 years of teaching experience. Her research interests include Signal processing for communication, Image processing, Signal processing using ML algorithms. Kavita Guddad has published more than 14 papers in journals/conferences of the International/National level.



K. L. Sudha received her B.E degree in Electronics and Communication Engineering and Master's degree in Electronics. Her research work on "Detection of FH CDMA signals in time varying channel" acquired her Ph.D from Osmania University, Hyderabad. She is working as Professor in the Department of Electronics and Communication Engineering, Dayananda Sagar College of Engineering, Bengaluru. She has worked in various reputed engineering colleges and gained more than 28 years of teaching experience. Her research interests include wireless communication, Channel coding, chaotic signal applications, image processing and signal processing. Six research scholars have secured doctorate degree under her guidance. Dr. K L Sudha has successfully completed 3 ISRO funded projects. She has published more than 120 papers in journals/conferences under the International and National level.

How to cite this paper:

Kavita Guddad, K. L. Sudha, "PLL based IRNSS Signal Tracking using Real Time Data", International Journal of Image, Graphics and Signal Processing(IJIGSP), Vol.18, No.5, pp. 93-109, 2026. DOI:10.5815/ijigsp.2026.05.06